Molecular Biophysics:

Extracellular Calcium Modulates Actions of Orthosteric and Allosteric Ligands on Metabotropic Glutamate Receptor 1α

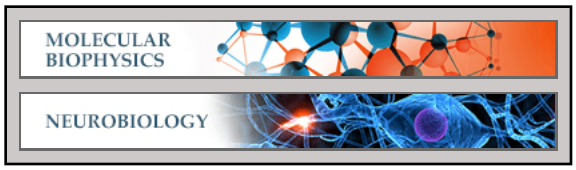

Jason Y. Jiang, Mulpuri Nagaraju, Rebecca C. Meyer, Li Zhang, Donald Hamelberg, Randy A. Hall, Edward M. Brown, P. Jeffrey Conn and Jenny J. Yang

J. Biol. Chem. 2014, 289:1649-1661.
doi: 10.1074/jbc.M113.507665 originally published online November 26, 2013

THE JOURNAL OF BIOLOGICAL CHEMISTRY VOL. 289, NO. 3, pp. 1649–1661, January 17, 2014

Extracellular Calcium Modulates Actions of Orthosteric and Allosteric Ligands on Metabotropic Glutamate Receptor 1α*

Received for publication, August 9, 2013, and in revised form, November 20, 2013 Published, JBC Papers in Press, November 26, 2013, DOI 10.1074/jbc.M113.507665

Jason Y. Jiang[‡], Mulpuri Nagaraju[‡], Rebecca C. Meyer[§], Li Zhang[‡], Donald Hamelberg[‡], Randy A. Hall[§], Edward M. Brown[¶], P. Jeffrey Conn[‖], and Jenny J. Yang[‡1]

From the [‡]Department of Chemistry, Center for Diagnostics and Therapeutics, Georgia State University, Atlanta, Georgia 30303, [§]Department of Pharmacology, Emory University School of Medicine, Atlanta, Georgia 30322, [¶]Division of Endocrinology, Diabetes and Hypertension, Department of Medicine, Brigham and Women's Hospital, Boston, Massachusetts 02115, and [‖]Department of Pharmacology, Vanderbilt University Medical Center, Nashville, Tennessee 37232

Background: Extracellular Ca^{2+} alters mGluR1α activity but by an unknown mechanism.
Results: Mutations in predicted Ca^{2+}-binding sites modulated the potency of both orthosteric and allosteric modulators.
Conclusion: Ca^{2+} binding exerts multiple types of effects on mGluR1α.
Significance: Improved knowledge of the mechanisms underlying the actions of Ca^{2+} on mGluR1α activity could facilitate development of isoform-selective drugs and/or suggest ways to tune the actions of available drugs.

Metabotropic glutamate receptor 1α (mGluR1α), a member of the family C G protein-coupled receptors, is emerging as a potential drug target for various disorders, including chronic neuronal degenerative diseases. In addition to being activated by glutamate, mGluR1α is also modulated by extracellular Ca^{2+}. However, the underlying mechanism is unknown. Moreover, it has long been challenging to develop receptor-specific agonists due to homologies within the mGluR family, and the Ca^{2+}-binding site(s) on mGluR1α may provide an opportunity for receptor-selective targeting by therapeutics. In the present study, we show that our previously predicted Ca^{2+}-binding site in the hinge region of mGluR1α is adjacent to the site where orthosteric agonists and antagonists bind on the extracellular domain of the receptor. Moreover, we found that extracellular Ca^{2+} enhanced mGluR1α-mediated intracellular Ca^{2+} responses evoked by the orthosteric agonist L-quisqualate. Conversely, extracellular Ca^{2+} diminished the inhibitory effect of the mGluR1α orthosteric antagonist (*S*)-α-methyl-4-carboxyphenylglycine. In addition, selective positive (Ro 67-4853) and negative (7-(hydroxyimino)cyclopropa[*b*]chromen-1*a*-carboxylate ethyl ester) allosteric modulators of mGluR1α potentiated and inhibited responses to extracellular Ca^{2+}, respectively, in a manner similar to their effects on the response of mGluR1α to glutamate. Mutations at residues predicted to be involved in Ca^{2+} binding, including E325I, had significant effects on the modulation of responses to the orthosteric agonist L-quisqualate and the allosteric modulator Ro 67-4853 by extracellular Ca^{2+}. These studies reveal that binding of extracellular Ca^{2+} to the predicted Ca^{2+}-binding site in the extracellular domain of mGluR1α modulates not only glutamate-evoked signaling but also the actions of both orthosteric ligands and allosteric modulators on mGluR1α.

The eight subtypes of metabotropic glutamate receptors (mGluRs)[2] belong to family C of the G protein-coupled receptors (GPCRs) and possess a large extracellular domain (ECD), a transmembrane domain (TMD), and a cytosolic C-terminal tail. The mGluRs are widely expressed in the central nervous system and play critical roles in regulating neuronal excitability and synaptic plasticity at both excitatory and inhibitory synapses (1). Extensive structural studies have revealed that the endogenous agonist L-glutamate (L-Glu), the major excitatory neurotransmitter in the central nervous system, binds at the hinge region of the ECD within the Venus fly trap motif of the receptor to activate the protein. This subsequently stimulates phospholipase C and leads to accumulation of inositol trisphosphate and an increase of intracellular calcium concentration ($[Ca^{2+}]_i$) (2–4).

In recent years, mGluRs have received increasing interest as potential drug targets for the treatment of a range of psychiatric and neurological diseases (5) (see Fig. 1). The ligands targeting mGluRs can be classified as orthosteric agonists and antagonists as well as allosteric modulators. Orthosteric agonists and antagonists induce and attenuate, respectively, the activity of the receptor by competitively binding to the L-Glu-binding pocket. L-Quisqualate (L-Quis), the most potent agonist of mGluR1 reported to date (6, 7), has been speculated to share nearly the same binding pocket as L-Glu (8, 9). In contrast, (*S*)-MCPG is an analog of L-Glu and is a non-selective competitive

* This work was supported, in whole or in part, by National Institutes of Health Grants GM081749-01 (to J. J. Y.), DK078331 (to E. M. B.), and NS055179 (to R. A. H.). This work was also supported by a Brains and Behavior fellowship (to Y. J.).

[1] To whom correspondence should be addressed: Dept. of Chemistry, Georgia State University, 552 Natural Science Center, Atlanta, GA 30303. Tel.: 404-413-5520; Fax: 404-413–5551; E-mail: jenny@gsu.edu.

[2] The abbreviations used are: mGluR, metabotropic glutamate receptor; GPCR, G protein-coupled receptor; ECD, extracellular domain; PAM, positive allosteric modulator; NAM, negative allosteric modulator; L-Quis, L-quisqualate, L(+)-α-amino-3,5-dioxo-1,2,4-oxadiazolidine-2-propanoic acid; (*S*)-MCPG, (*S*)-α-methyl-4-carboxyphenylglycine; CPCCOEt, 7-(hydroxyimino)cyclopropa[*b*]chromen-1*a*-carboxylate ethyl ester; Ro 67-4853, (9*H*-xanthen-9-ylcarbonyl)carbamic acid butyl ester; TMD, transmembrane domain.

antagonist that has been shown to occupy the L-Glu-binding pocket, thereby blocking the function of group I/II members in the mGluR family (10). On the other hand, allosteric modulators bind to sites other than the orthosteric center to affect the activity of the receptor. Ro 67-4853 is a positive allosteric modulator (PAM) of mGluR1 that enhances the potency of L-Glu by interacting with the TMD of the receptor. CPCCOEt is a negative allosteric modulator (NAM) that inhibits the activation of mGluR1 by L-Glu by specifically binding to a site that involves the third extracellular loop of mGluR1α (11).

Like other members of the family C GPCRs, such as the calcium-sensing receptor, mGluR1α senses $[Ca^{2+}]_o$ using the extracellular domain (12, 13). By transient expression of mGluR1α in oocytes, Kubo *et al.* (4) demonstrated that mGluR1-mediated activation of Ca^{2+}-activated Cl^- channels is modulated by $[Ca^{2+}]_o$ in addition to L-Glu. Purkinje cells from mGluR1 knock-out mice lose sensitivity to $[Ca^{2+}]_o$, and this sensitivity to $[Ca^{2+}]_o$ was restored after mGluR1 was genetically reintroduced into the mice (14). There are sparse reports of $[Ca^{2+}]_o$ affecting the action of various classes of compounds acting on mGluRs (15). However, it is not clear how $[Ca^{2+}]_o$ is able to modulate the activity of mGluR1 or the actions of various mGluR1 ligands, and no Ca^{2+}-binding sites have been identified in the 15 structures solved by x-ray crystallography to date (Protein Data Bank).

Using our recently developed computational algorithm, we identified a novel potential $[Ca^{2+}]_o$-binding site within the hinge region of the ECD of mGluR1α adjacent to the reported L-Glu-binding site (16, 17). It comprises Asp-318, Glu-325, Asp-322, and the carboxylate side chain of the natural agonist L-Glu. The carboxylate side chains of both L-Glu and Asp-318 are involved in both L-Glu and $[Ca^{2+}]_o$ binding. Our previous mutagenesis study indicated that binding of L-Glu and Ca^{2+} to their distinct but partially overlapping binding sites synergistically modulates mGluR1α-mediated activation of $[Ca^{2+}]_i$ signaling. Mutating the L-Glu-binding site completely abolished L-Glu signaling but left its Ca^{2+}-sensing capability largely intact. Mutating predicted Ca^{2+}-binding residues not only abolished or significantly reduced the sensitivity of mGluR1α to $[Ca^{2+}]_o$ but also in some cases to L-Glu (18).

In the present study, we first demonstrated that our predicted Ca^{2+}-binding site is adjacent to the orthosteric agonist and antagonist interaction sites. We then examined the role of $[Ca^{2+}]_o$ in modulating the actions of different orthosteric ligands acting on mGluR1α, including L-Quis and (*S*)-MCPG as well as reciprocal interactions between Ca^{2+} and the mGluR1 allosteric modulators Ro 67-4853 and CPCCOEt. Our results suggest that $[Ca^{2+}]_o$ modulates the sensitivity of mGluR1α to not only orthosteric agonists and antagonists but also to allosteric modulators likely by interacting with the predicted $[Ca^{2+}]_o$-binding site in the ECD of the receptor.

EXPERIMENTAL PROCEDURES

Docking L-Quis to ECD-mGluR1α Using AutoDock Vina and Hinge Motion Analysis—To elucidate binding of L-Quis to the ECD of mGluR1α, L-Quis was docked into the crystal structure (Protein Data Bank 1EWK). After removing the coordinates of the bound endogenous ligand, L-Glu, the Protein Data Bank file was loaded into AutoDock tools to add polar hydrogen atoms and choose the docking center and grid box. The docking work was carried out by the AutoDock tool Vina (Scripps). The binding residues were analyzed by measuring the atoms within 6 Å of L-Quis. The L-Glu- and the (*S*)-MCPG-binding sites within the hinge region were analyzed using Dymdon.

Molecular Dynamics Simulation and Correlation Analysis Using AMBER—The initial coordinates for all the simulations were taken from a 2.20-Å resolution x-ray crystal structure (Protein Data Bank code 1EWK; Ref. 19). The AMBER 10 suite of programs (20) was used to carry out all of the simulations in an explicit TIP3P (transferable intermolecular potential 3P) water model (21) using the modified version of the all-atom Cornell *et al.* (22) force field and the reoptimized dihedral parameters for the peptide ω-bond (23). The crystal structure contains only Glu substrate. Ca^{2+} ion was placed at the suggested Ca^{2+}-binding site that is defined by residues Asp-318, Asp-322, and Glu-325. An initial 2-ns simulation was performed using NOE restraint during the equilibration to reorient the side chain residues in the Ca^{2+}-binding site, but no restraints were used during the actual simulation. A total of four molecular dynamics simulations were carried out for 50 ns each on wild type and three mutant mGluRs. The mutations were D318I, D322I, and E325I. First, our structures were minimized to achieve the lowest energy conformation in each complex. The structures were then equilibrated for 2 ns, starting the molecular dynamics simulations from the equilibrated structures. During the simulations, an integration time step of 0.002 ps was used to solve Newton's equation of motion. The long range electrostatic interactions were calculated using the particle mesh Ewald method (24), and a cutoff of 9.0 Å was applied for non-bonded interactions. All bonds involving hydrogen atoms were restrained using the SHAKE algorithm (25). The simulations were carried out at a temperature of 300 K and a pressure of 1 bar. A Langevin thermostat was used to regulate the temperature with a collision frequency of 1.0 ps^{-1}. The trajectories were saved every 500 steps (1 ps). The trajectories were then analyzed using the ptraj module in AMBER 10.

Constructs, Site-directed Mutagenesis, and Expression of mGluR1α Variants—The red fluorescent protein mCherry was genetically tagged to the C terminus of mGluR1α by a flexible linker, GGNSGG (18). Point mutations were introduced using a site-directed mutagenesis kit (Stratagene). HEK293 cells were seeded and cultured on glass coverslips. mGluR1α and its mutants were transfected into cells utilizing Lipofectamine 2000 (Invitrogen). The cells were then incubated for an additional 2 days so that mGluR1α and its mutants were expressed at sufficient levels for study. Cells were fixed on the coverslips with 4% formaldehyde, and nuclei were stained with DAPI. The expression of mGluR1α and its variants was detected by measuring red fluorescence using confocal microscopy at 587 nm.

Determining the Effect of $[Ca^{2+}]_o$ on Activation of mGluR1α and Its Mutants by L-Quis—Measurement of $[Ca^{2+}]_i$ was performed as described (13). In brief, wild type mGluR1α was transiently transfected into the cells and cultured for an additional 2 days. The cells on the coverslips were subsequently loaded using 4 μM Fura-2 AM in 2 ml of physiological saline buffer (10 mM HEPES, 140 mM NaCl, 5 mM KCl, 0.55 mM $MgCl_2$, and 1 mM

$CaCl_2$, pH 7.4) for 30 min. The coverslips were then mounted in a bathing chamber on the stage of a fluorescence microscope at room temperature. Fura-2 emission signals at 510 nm from single cells excited at 340 or 380 nm were collected utilizing a Leica DM6000 fluorescence microscope in real time as the concentration of L-Quis was progressively increased in the presence or absence of $[Ca^{2+}]_o$. The ratio of fluorescence emitted at 510 nm resulting from excitation at 340 or 380 nm was further analyzed to obtain the $[Ca^{2+}]_i$ response as a function of changes in L-Quis. Only the individual cells expressing mCherry were selected for analysis.

Measurement of $[Ca^{2+}]_i$ Responses of mGluR1α to $[Ca^{2+}]_o$ or L-Glu in the Presence of 0.5 mM (S)-MCPG—The methods for measuring $[Ca^{2+}]_i$ responses were as described above. In the presence of (*S*)-MCPG, the cells were incubated with 0.5 mM (*S*)-MCPG in a L-Glu-free saline buffer for 30 more min after Fura-2 loading. Then the sensitivity of mGluR1α to $[Ca^{2+}]_o$ or added L-Glu was measured either by increasing the concentration of L-Glu in the presence of 1.8 mM $[Ca^{2+}]_o$ or by increasing $[Ca^{2+}]_o$ in a stepwise manner in the saline buffer with or without 0.5 mM (*S*)-MCPG. The L-Glu concentrations were recorded when the $[Ca^{2+}]_i$ responses of mGluR1α were first observed and then were saturated.

Determining the Effects of $[Ca^{2+}]_o$ on the Potency of Ro 67-4853 on mGluR1α—Fura-2 AM was used for monitoring $[Ca^{2+}]_i$ in real time as described above. Ro 67-4853 did not potentiate mGluR1α in the absence of L-Glu (26, 27). To obtain the $[Ca^{2+}]_i$ readout, HEK293 cells expressing mGluR1α were preincubated with 0.5 mM Ca^{2+} and 5 nM Ro 67-4853 for at least 10 min. Cells loaded with Fura-2 AM were mounted onto a chamber perfused with saline buffer. The concentration of Ro 67-4853 was increased stepwise in the presence of 0.5 or 1.8 mM $[Ca^{2+}]_o$, and $[Ca^{2+}]_i$ was recorded as before by the ratiometric change of Fura-2 AM in response to changes in $[Ca^{2+}]_i$. The effect of $[Ca^{2+}]_o$ was analyzed by comparing the intracellular Ca^{2+} responses elicited by Ro 67-4853 at two different concentrations of Ca^{2+} in the perfusion buffer. To determine the effect of Ro 67-4853 on the sensitivity of mGluR1α to $[Ca^{2+}]_o$, an additional 30 or 300 nM Ro 67-4853 was applied as $[Ca^{2+}]_o$ was increased.

Measurement of $[Ca^{2+}]_i$ Responses of mGluR1α to $[Ca^{2+}]_o$ or L-Glu in the Presence of CPCCOEt—After the coverslip was mounted in the microscope, the cells were perfused with a saline buffer containing 0, 5, or 40 μM CPCCOEt for more than 10 min. Increasing concentrations of $[Ca^{2+}]_o$ or L-Glu were added to the chamber in the presence of varying concentrations of CPCCOEt, and the $[Ca^{2+}]_i$ response was recorded.

Determining the Effects of $[Ca^{2+}]_o$ on L-[^{3}H]Quis Binding to mGluR1α and Its Mutants—HEK293 cells transiently transfected with wild type mGluR1α or its mutants were maintained in a 5% CO_2 37 °C incubator for an additional 48 h as before. Cells were then collected in ice-cold hypotonic buffer (20 mM HEPES, 100 mM NaCl, 5 mM $MgCl_2$, 5 mM KCl, 0.5 mM EDTA, and 1% protease inhibitors at pH 7.0–7.5). The cell pellet was washed twice more using hypotonic buffer to remove the L-Glu in the cellular debris. The crude membrane protein (100 μg) was mixed with 30 nM L-[^{3}H]Quis in 100 μl of hypotonic buffer. The nonspecific binding was determined by measuring bound L-[^{3}H]Quis in the presence of 200 μM L-Glu. To study the effects of $[Ca^{2+}]_o$ on L-Quis binding to mGluR1α, increasing concentrations of $[Ca^{2+}]_o$ were applied. The reaction mixtures were incubated on ice for at least 1 h, and the membrane-bound L-[^{3}H]Quis was captured on filter paper using a Brandel cell harvester under vacuum. The filter paper was then transferred to scintillation fluid, and L-[^{3}H]Quis was detected using a Beckman LS 6500 multipurpose scintillation counter.

RESULTS

Predicted $[Ca^{2+}]_o$-binding Site Is Adjacent to Orthosteric Agonist and Antagonist-binding Sites—Using our recently developed computational algorithms, we have identified a novel potential Ca^{2+}-binding site at the hinge region of the ECD of mGluR1α (18). Fig. 1 shows that the predicted Ca^{2+}-binding site comprises Asp-318, Glu-325, Asp-322, and the carboxylate side chain of the natural agonist L-Glu in the hinge region in the ECD of mGluR1α adjacent to the reported L-Glu-binding site. Asp-318 is involved in both L-Glu and Ca^{2+} binding (18).

Using the crystal structure (Protein Data Bank code 1EWK; closed-open form) of the ECD of the receptor and the AutoDock Vina program, we modeled the binding site for the orthosteric agonist L-Quis. As shown in Fig. 1*B*, the docked binding site of the agonist L-Quis corresponds well with the L-Glu-binding residues previously suggested by the crystal structure. Our predicted Ca^{2+}-binding site is also adjacent to the L-Quis pocket and interacts with L-Quis similarly to L-Glu (Fig. 1*B*). In the reported crystal structure of mGluR1 complexed with an orthosteric antagonist, (*S*)-MCPG (Protein Data Bank code 1ISS), (*S*)-MCPG interacts with Tyr-74, Trp-110, Ser-165, Thr-188, and Lys-409 in lobe 1 and Asp-208, Tyr-236, and Asp-318 in lobe 2 (Fig. 1*B*) (10). It shares with L-Glu most of the residues of the L-Glu-binding pocket (10) and is also adjacent to our predicted Ca^{2+}-binding site.

We next performed molecular dynamics simulations to reveal any possible interaction between our predicted $[Ca^{2+}]_o$-binding site and the orthosteric ligand-binding site. Residues involved in the $[Ca^{2+}]_o$-binding pocket, such as Asp-318, Asp-322, and Glu-325, have strong correlated motions as expected given their roles as $[Ca^{2+}]_o$-binding ligands. In addition, residues Asp-318 and Arg-323 residing within the same loop as the predicted Ca^{2+}-binding site are also concurrently correlated. As shown in Fig. 2, most of the critical L-Glu-binding residues, including Trp-110, Ser-165, Thr-188, Asp-208, Tyr-236, Asp-318, and Arg-323, are well correlated to the $[Ca^{2+}]_o$-binding site (Asp-318, Asp-322, and Glu-325). However, mutations at the charged residues involved in $[Ca^{2+}]_o$ binding, such as D318I and E325I, markedly attenuated the correlation of the Ca^{2+}-binding site with the L-Glu-binding pocket. The Ca^{2+}-binding site in mutant D318I only correlates with Gly-293 and Asp-208, and mutant D325I only correlates with Tyr-236 and Gly-293. The mutant D322I also exhibited impaired correlation between the $[Ca^{2+}]_o$-binding site and L-Glu-binding site but to a lesser degree. As shown in Table 1, Asp-318 in the $[Ca^{2+}]_o$-binding site still correlates with four residues in the L-Glu-binding pocket (Fig. 2). Similarly, residues that are involved in binding L-Quis and (*S*)-MCPG also correlate well with residues

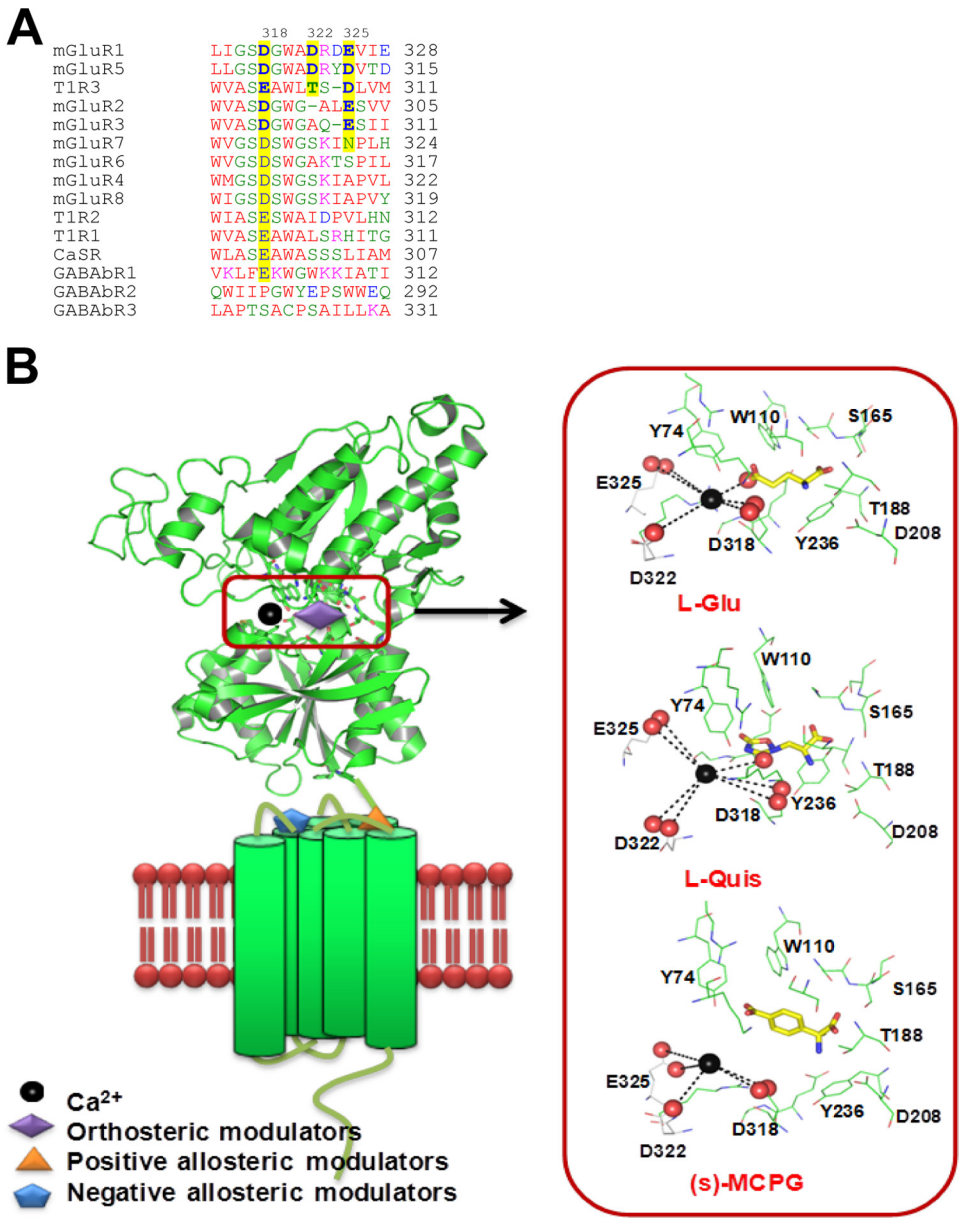

FIGURE 1. **Schematic view of the binding sites for $[Ca^{2+}]_o$, L-Glu, L-Quis, and (*S*)-MCPG in the mGluR1α ECD.** *A*, the $[Ca^{2+}]_o$-binding site is highly conserved in group I mGluRs and T1R3. In contrast, although sequence alignment suggests that the $[Ca^{2+}]_o$-binding site is highly conserved in group I mGluRs, it is not conserved in other members of the subfamily. *B*, L-Glu, L-Quis, and (*S*)-MCPG-binding pockets (*purple diamond*) and scheme of binding sites for various classes of ligands acting on mGluR1α. Similar to the L-Glu-binding pocket, Tyr-74, Arg-78, Ser-165, Thr-188, Tyr-236, Asp-318, and Lys-409 form the L-Quis-binding pocket. Similar residues, Tyr-74, Trp-110, Ser-165, Thr-188, Tyr-236, Asp-318, and Lys-409, that contribute to the L-Glu-binding pocket are also involved in binding of (*S*)-MCPG. L-Glu, L-Quis, and (*S*)-MCPG wedge into a location adjacent to the $[Ca^{2+}]_o$-binding site in the ECD and maintain the structure of the receptor in its active and resting forms, respectively. The residues with more than one *dotted line* indicate those that have more than one oxygen atom contributing to ligand binding. Most of the positive (*orange triangle*) and negative (*cyan pentagon*) allosteric modulators have been discovered to bind to TMDs but do not share the same binding site.

involved in the predicted $[Ca^{2+}]_o$-binding site. Results from these analyses and our previous studies on the effect of binding of $[Ca^{2+}]_o$ to its site on L-Glu-mediated activation of mGluR1 led us to hypothesize that $[Ca^{2+}]_o$ regulates the effects of orthosteric ligands on mGluR1α.

Ca^{2+} Enhances Sensitivity of Activation of mGluR1α by L-Quis by Increasing L-[^{3}H]Quis Binding via Interaction with the $[Ca^{2+}]_o$-binding Site of the Receptor—To test the effect of $[Ca^{2+}]_o$ on the activation of mGluR1α by the orthosteric agonist L-Quis, we performed a single cell fluorescence imaging assay by measuring changes in $[Ca^{2+}]_i$ using HEK293 cells transiently transfected with mGluR1α and loaded with Fura-2. To eliminate any potential effect of trace L-Glu secreted from cells, experiments were conducted using continuous superfusion of cells with an L-Glu-free buffer. Fig. 3, *A–D*, show that L-Quis induced intracellular calcium responses mediated by mGluR1 in a manner similar to the activation of the receptor by L-Glu. $[Ca^{2+}]_o$ behaved as a PAM of the L-Quis response and induced a leftward shift in the L-Quis concentration-response curve for activation of mGluR1a (Fig. 3, *A–D*). In the absence of $[Ca^{2+}]_o$ (Ca^{2+}-free buffer with less than 2 μM calcium), the EC_{50} for the activation of mGluR1a by L-Quis is 12.8 nM. The addition of 1.8

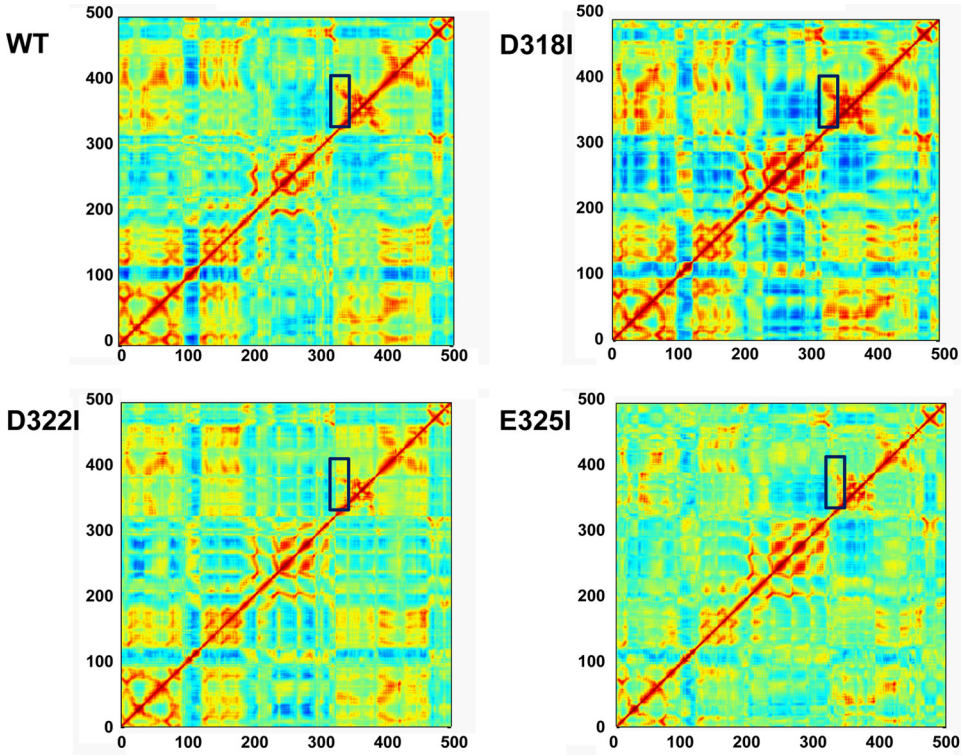

FIGURE 2. **Correlation maps of WT mGluR1α and D318I, D322I, and E325I.** The predicted $[Ca^{2+}]_o$-binding site is well correlated to the L-Glu-binding pocket. Mutations of the $[Ca^{2+}]_o$-binding site impair the correlation to the L-Glu-binding pocket. The $[Ca^{2+}]_o$-binding site corresponding to the *x axis* is highlighted by a *rectangle*.

TABLE 1

Mutations in the $[Ca^{2+}]_o$-binding site perturb the correlated motions between the $[Ca^{2+}]_o$-binding site and the L-Glu-binding site of mGluR1α

Based on the correlation map shown in Fig. 2, there is correlated motion between the reported L-Glu-binding pocket and the $[Ca^{2+}]_o$-binding site (Asp-318, Asp-322, and Glu-325). The residues with absolute correlation values greater than 0.3 are listed in this table. Of note, WT has five residues (bold residues are not included because they reside in the same loop as the $[Ca^{2+}]_o$-binding site and thus would have the same motion) in the L-Glu-binding site that correlate with $[Ca^{2+}]_o$-binding site, whereas there are only correlations between two residues in variants D318I and E325I and four in D322I. Bold residues are in the same loop as the $[Ca^{2+}]_o$-binding site, and they have the same movements as the $[Ca^{2+}]_o$-binding site by default.

	Asp-318	Asp-322	Glu-325
WT	Trp-110, Ser-165, Thr-188, Asp-208, Tyr-236, **Asp-318**, **Arg-323**	Trp-110, Ser-165, Thr-188, Tyr-236, **Asp-318**, **Arg-323**	**Arg-323**
D318I	Asp-208, Gly-293, **Asp-318**, **Arg-323**	Gly-293, **Asp-318**, **Arg-323**	Gly-293, **Asp-318**, **Arg-323**
D322I	Tyr-74, Trp-110, Gly-293, **Asp-318**, **Arg-323**, Lys-409	**Asp-318**, **Arg-323**	Tyr-74, Gly-293, **Asp-318**, **Arg-323**
E325I	Tyr-236, Gly-293, **Asp-318**, **Arg-323**	Gly-293, **Asp-318**, **Arg-323**	Gly-293, **Asp-318**, **Arg-323**

mM $[Ca^{2+}]_o$ reduced the EC_{50} of L-Quis to 2.8 nM (about 4.6-fold) (Fig. 3*D* and Table 2). This $[Ca^{2+}]_o$-mediated increase in the potency of L-Quis is similar to the effect of $[Ca^{2+}]_o$ on the activation of mGluR1 by its natural agonist L-Glu (18).

To test whether this $[Ca^{2+}]_o$-mediated increase in the potency of L-Quis occurs via our predicted $[Ca^{2+}]_o$-binding site in the ECD of the receptor, we then examined three mGluR1 variants with mutations around the $[Ca^{2+}]_o$-binding site adjacent to the orthosteric binding site at the hinge region. The negatively charged side chain of Glu-325 has previously been shown to be important for $[Ca^{2+}]_o$ binding by mGluR1 and not directly involved in L-Glu binding (18). Removal of the $[Ca^{2+}]_o$-binding ligand residue Glu-325 in the mGuR1 variant E325I reduced potency, increasing the EC_{50} from 12.6 to 20 nM in the absence of $[Ca^{2+}]_o$ (Fig. 3*D* and Table 2). Importantly, this mutation significantly reduced the $[Ca^{2+}]_o$-mediated enhancement in potency for L-Quis from 4.6- to 1.6-fold in 1.8 mM $[Ca^{2+}]_o$, although both the potency and efficacy of L-Quis-mediated activation of the E325I mutant were still enhanced relative to WT mGluR1 (Fig. 3, *A–D*). As L-Glu could potentially serve as a ligand for binding of Ca^{2+} to its pocket, L-Glu or L-Quis binding could rescue the mutated Ca^{2+}-binding pocket, thus enhancing the Ca^{2+} sensitivity of the mutant. On the other hand, mutant D322I exhibited WT-like behavior in its response to L-Quis both in the absence and presence of $[Ca^{2+}]_o$ (Fig. 3, *A–D*, and Table 2), consistent with Asp-322 contributing to $[Ca^{2+}]_o$ binding to a lesser degree with only its main chain oxygen serving as a ligand atom. We also observed WT-like modulation of the L-Glu response of D332I by Ca^{2+} (18). These $[Ca^{2+}]_i$ imaging data suggest that $[Ca^{2+}]_o$ plays a key role in modulating the activation of mGluR1α by L-Quis, possibly via interaction of $[Ca^{2+}]_o$ at the predicted $[Ca^{2+}]_o$-binding site.

We utilized a direct binding assay with radioactive L-Quis (L-[^{3}H]Quis) to assess the impact of $[Ca^{2+}]_o$ on the binding of L-[^{3}H]Quis to mGluR1α or its variants with mutations at the predicted $[Ca^{2+}]_o$-binding ligand residues in the absence or presence of $[Ca^{2+}]_o$. L-Quis binds to the wild type receptor expressed in HEK293 with a k_d in the range of 30 nM. L-Glu

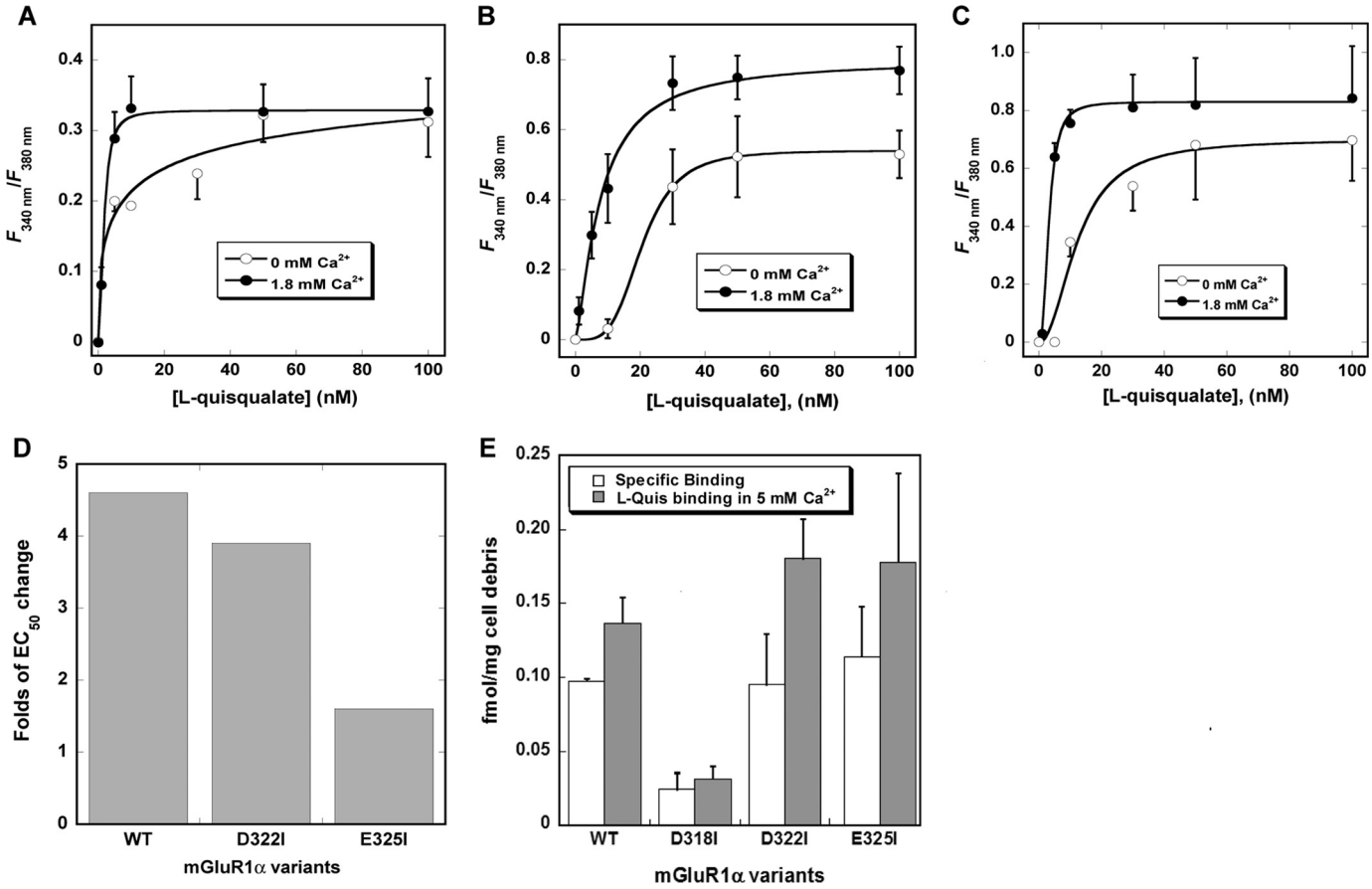

FIGURE 3. **Extracellular Ca^{2+} enhances L-Quis activation of mGluR1α by binding to the predicted $[Ca^{2+}]_o$-binding site.** *A–C*, addition of 1.8 mM $[Ca^{2+}]_o$ (*solid circles*) increases the L-Quis-induced $[Ca^{2+}]_i$ responses mediated by activation of mGluR1α. The response with 0 mM $[Ca^{2+}]_o$ is indicated by the *empty circles*. In the presence of 1.8 mM $[Ca^{2+}]_o$, the L-Quis sensitivity of D322I was increased. 1.8 mM $[Ca^{2+}]_o$ also enhanced the potency of L-Quis on E325I. *D*, the -fold change in EC_{50} for activation of WT mGluR1α, D322I, and E325I by L-Quis upon increasing $[Ca^{2+}]_o$ from nominal 0 to 1.8 mM. The -fold decreases in the EC_{50} values for WT mGluR1α, D322I, and E325I are 4.6, 3.9, and 2.7, respectively. *E*, L-[^{3}H]Quis binds to WT mGluR1α in the absence of $[Ca^{2+}]_o$, but mutations in the $[Ca^{2+}]_o$-binding site decrease L-Quis binding. D318I eliminated L-Quis binding, whereas D322I and E325I still retained L-Quis binding. An additional 5 mM $[Ca^{2+}]_o$ enhanced L-Quis binding to WT mGluR1α ($p = 0.031$) and D322I, whereas this $[Ca^{2+}]_o$ effect was abolished in E325I. The binding buffer used was hypotonic buffer ($n = 3$) (*, $p < 0.05$). *Error bars* represent S.D.

TABLE 2

Effects of $[Ca^{2+}]_o$ on the responses of WT mGluR1α and variants with mutations of $[Ca^{2+}]_o$-binding site to L-Quis

$[Ca^{2+}]_i$ response increases induced by increasing L-Quis via WT mGluR1a, D322I, and E325I were measured in both Ca^{2+}-free saline and buffer with physiological Ca^{2+}.

	WT			D322I			E325I		
	EC_{50}	Maximal response[a]	-Fold decrease in EC_{50}	EC_{50}	Maximal response[a]	-Fold decrease in EC_{50}	EC_{50}	Maximal response[a]	-Fold decrease in EC_{50}
	nM	%		*nM*	%		*nM*	%	
$[Ca^{2+}]_o$ concentration									
0 mM	12.8	37 ± 4	4.6	12.4	80 ± 16	3.9	20.6	60 ± 8	2.7
1.8 mM	2.8	37 ± 5		3.2	96 ± 21		7.6	88 ± 8	
K_d (mM)[b]	0.3			0.6			>20.0		

[a] The maximal responses are normalized to the maximal response of WT mGluR1α to L-Glu.
[b] $[Ca^{2+}]_o$ binding affinity of mGluR1α in the presence of 30 nM L-[^{3}H]Quis (E325I with 300 nM L-[^{3}H]Quis).

reduced L-Quis binding by competing for the similar orthosteric binding pocket (Figs. 1*B* and 4*B*, *inset*). $[Ca^{2+}]_o$ significantly enhanced L-Quis binding to the wild type receptor with an EC_{50} in the range of 0.3 mM (Fig. 3*E* and Table 2). Variant E325I with removal of negative charge on the key $[Ca^{2+}]_o$-binding residue Glu-325 abolished L-Quis binding, and this effect was not influenced by the addition of L-Glu or $[Ca^{2+}]_o$ ($K_d > 20$ mM) (Table 2). On the other hand, variant D322I retained the binding properties of the wild type receptor for L-Quis, suggesting that it has a less essential role in L-Quis binding (Fig. 3*E*), which is consistent with its role in activation of the $[Ca^{2+}]_i$ responses described earlier. Taken together, both the studies of $[Ca^{2+}]_i$ responses and L-Quis binding suggest that $[Ca^{2+}]_o$ enhances the activation of mGluR1 by L-Quis by directly modulating binding of L-Quis to mGluR1 through an interaction with predicted $[Ca^{2+}]_o$-binding site 1 in the hinge region.

(S)-MCPG Reduces the Sensitivity of mGluR1α to L-Glu and $[Ca^{2+}]_o$—The effects of $[Ca^{2+}]_o$ on various mGluR1 ligands acting by different mechanisms on mGluR1 were evaluated

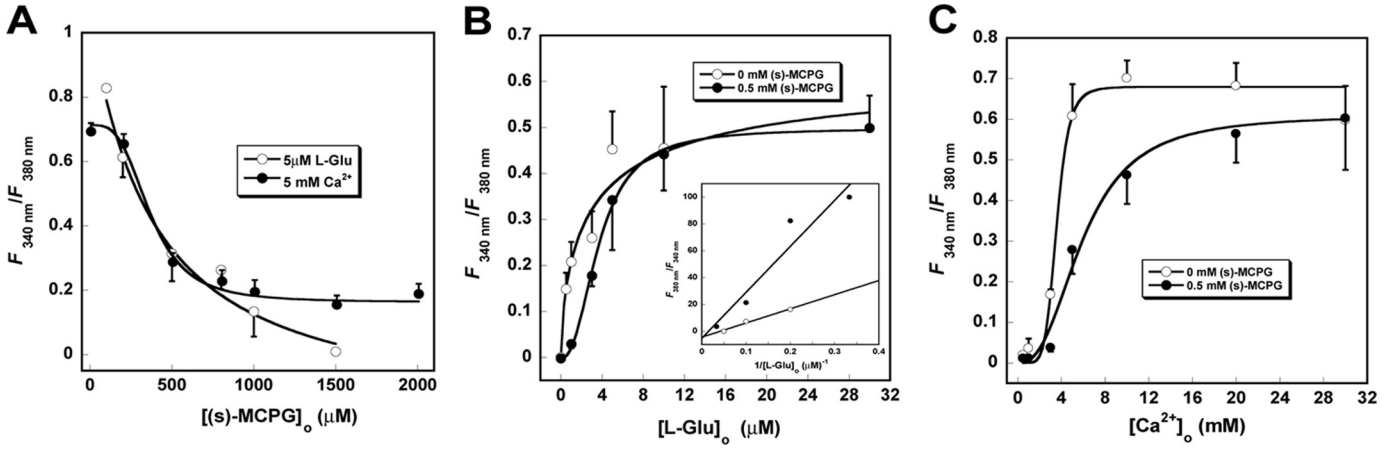

FIGURE 4. **Effects of (*S*)-MCPG on the response of WT mGluR1α to L-Glu and $[Ca^{2+}]_o$.** *A*, increasing the concentration of (*S*)-MCPG inhibits mGluR1α in the presence of 5 μM L-Glu, and 1.5 mM (*S*)-MCPG entirely blocks the activation of the receptor by L-Glu. (*S*)-MCPG attenuated the responsiveness of mGluR1α to 5 mM $[Ca^{2+}]_o$, and 2.0 mM (*S*)-MCPG did not completely inhibit the capacity of the receptor to sense $[Ca^{2+}]_o$. *B*, 0.5 mM (*S*)-MCPG competitively inhibits L-Glu-induced $[Ca^{2+}]_i$ responses. Lineweaver-Burk plot analysis indicated that (*S*)-MCPG competes with L-Glu (*inset*). *C*, 0.5 mM (*S*)-MCPG inhibits low $[Ca^{2+}]_o$-induced $[Ca^{2+}]_i$ responses, but high $[Ca^{2+}]_o$ restores the response of the receptor ($n = 3$). *Error bars* represent S.D.

TABLE 3

Addition of 0.5 mM (S)-MCPG decreases the responses of mGluR1α to $[Ca^{2+}]_o$ and L-Glu

The $[Ca^{2+}]_i$ response to $[Ca^{2+}]_o$ and L-Glu in the absence or presence of 0.5 mM (*S*)-MCPG were obtained by measuring the ratiometric change of Fura-2 AM fluorescence.

	Response to $[Ca^{2+}]_o$			Response to L-Glu	
(*S*)-MCPG	EC_{50}	n_{Hill}	Maximal response[a]	EC_{50}	Maximal response[a]
mM	mM		%	μM	%
0	3.5	6.4	85 ± 2	1.7	100 ± 2
0.5	6.0	2.6	67 ± 2	3.7	97 ± 5

[a] The maximal responses are normalized to the maximal response of WT mGluR1α to L-Glu.

using L-Glu as the orthosteric agonist because it is the physiological activator of the receptor *in vivo*. As shown in Fig. 4, (*S*)-MCPG induced a concentration-dependent decrease in the L-Glu-evoked $[Ca^{2+}]_i$ response (Fig. 4*A*). A concentration of 0.5 mM (*S*)-MCPG elicited a parallel rightward shift in the L-Glu concentration-response curve and increased the EC_{50} for L-Glu from 1.7 to 3.7 μM. This is consistent with the known action of (*S*)-MCPG as a competitive antagonist at the orthosteric L-Glu-binding site.

Interestingly, Fig. 4*A* shows that (*S*)-MCPG also induced a concentration-dependent inhibition of the 5 mM $[Ca^{2+}]_o$-induced $[Ca^{2+}]_i$ response even in the absence of added L-Glu. Unlike the effect of (*S*)-MCPG on the response to L-Glu, (*S*)-MCPG did not completely block the response to $[Ca^{2+}]_o$. This is consistent with the hypothesis that (*S*)-MCPG inhibits the response to $[Ca^{2+}]_o$ by acting at a site distinct from the site that allosterically regulates the response to $[Ca^{2+}]_o$. (*S*)-MCPG also induced a rightward shift in the $[Ca^{2+}]_o$ concentration-response curve. The EC_{50} for $[Ca^{2+}]_o$ increased by ~1.7-fold (from 3.5 to 6.0 mM at 0 and 0.5 mM (*S*)-MCPG, respectively) (Fig. 4*C* and Table 3). The maximal response to $[Ca^{2+}]_o$ was not affected by 0.5 mM (*S*)-MCPG. However, as noted above, higher concentrations of (*S*)-MCPG could not fully block the maximal effect of 5 mM $[Ca^{2+}]_o$.

NAM CPCCOEt Non-competitively Inhibits Both L-Glu-induced and $[Ca^{2+}]_o$-induced Activation of mGluR1α—CPCCOEt is known as a selective, non-competitive NAM of mGluR1 that binds to residues Thr-815 and Ala-818 in the seventh TMD of the receptor (28) (Fig. 1). As shown in Fig. 5*A*, the L-Glu-triggered $[Ca^{2+}]_i$ response was significantly depressed in the presence of 5 and 40 μM CPCCOEt. In the presence of 40 μM CPCCOEt, the maximal response decreased to only about half of the control level, whereas the EC_{50} value increased from 1.7 to 10.1 μM (Fig. 5*A* and Table 4). To determine the effects of CPCCOEt on the activation of mGluR1α by $[Ca^{2+}]_o$, we next examined the effect of CPCCOEt on $[Ca^{2+}]_o$-induced $[Ca^{2+}]_i$ responses. Fig. 5*B* reveals that CPCCOEt significantly inhibited the $[Ca^{2+}]_o$ sensitivity of mGluR1α. In the presence of 5 μM CPCCOEt, the EC_{50} of mGluR1α for $[Ca^{2+}]_o$ was increased from 3.5 to 14.7 mM. A concentration of 40 μM CPCCOEt produced an even higher EC_{50} value of 28.7 mM (Fig. 5*B* and Table 4). The maximal response was also significantly decreased by 40 μM CPCCOEt, although the maximal response with 5 μM CPCCOEt was still comparable. This indicates that 30 mM $[Ca^{2+}]_o$ cannot completely reverse the antagonism induced by CPCCOEt, and thus the inhibitory effects of CPCCOEt on the response of mGluR1α to $[Ca^{2+}]_o$ appear to be non-competitive (Fig. 5*B* and Table 4).

The mGluR1α PAM Ro 67-4853 Potentiates Activation of mGluR1 by $[Ca^{2+}]_o$—The finding that CPCCOEt inhibited activation of mGluR1 by $[Ca^{2+}]_o$ suggests that the CPCCOEt site in the transmembrane-spanning domain of mGluR1 and the $[Ca^{2+}]_o$-binding site in the ECD of the receptor interact in a manner similar to the interactions between the orthosteric L-Glu-binding site and the allosteric CPCCOEt site. We performed analogous experiments to determine whether the mGluR1 PAM Ro 67-4853, which binds to the extracellular loops of the TMDs of mGluR1α (2, 29) (Fig. 1*B*), can also potentiate responses to $[Ca^{2+}]_o$. Fig. 6*A* shows that L-Glu-induced activation of WT mGluR1α was enhanced by the addition of 10 or 100 nM Ro 67-4853 using single cell $[Ca^{2+}]_i$ imaging. We then examined the effects of Ro 67-4853 on the $[Ca^{2+}]_o$ sensitivity of wild type mGluR1α in the absence of L-Glu. Fig. 6*B* shows that both 30 and 300 nM Ro 67-4853 enhanced the $[Ca^{2+}]_i$ response induced by $[Ca^{2+}]_o$, reducing the EC_{50} values for $[Ca^{2+}]_o$ from 3.5 mM to 2.1 and 0.7 mM, respectively. As with

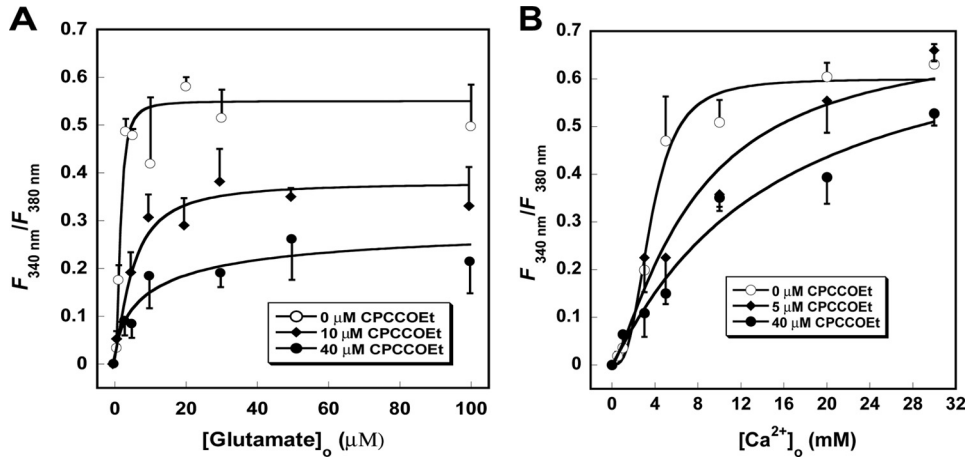

FIGURE 5. **Effects of CPCCOEt on the responses of mGluR1α to L-Glu and [Ca^{2+}]$_o$.** *A*, in the presence of 10 or 40 μM CPCCOEt, the sensitivity of mGluR1α to L-Glu was reduced. The maximal response was reduced to about 50% in the presence of 40 μM CPCCOEt. *B*, the [Ca^{2+}]$_o$ sensitivity of wild type mGluR1a was reduced by the addition of 5 or 40 μM CPCCOEt. [Ca^{2+}]$_i$ was measured using Fura-2 AM in the absence (*solid circles*) or presence of 5 (*solid diamonds*) or 40 μM (*empty circles*) CPCCOEt. In the cells inhibited by CPCCOEt (5 or 40 μM), increasing [Ca^{2+}]$_o$ counteracted the inhibitory effects of CPCCOEt. HEK293 cells transiently expressing WT mGluR1α were mounted on coverslips, and the [Ca^{2+}]$_i$ change indicated by Fura-2 AM was recorded ($n = 3$). *Error bars* represent S.D.

TABLE 4

The effects of CPCCOEt on the responsiveness of mGluR1α to L-Glu and [Ca^{2+}]$_o$ (n = 3)

WT mGluR1α was incubated with increasing concentrations (conc.) of [Ca^{2+}]$_o$ with either 0, 5, or 40 nM CPCCOEt (left side) or to increasing concentrations of L-Glu in the presence of the indicated fixed concentrations of CPCCOEt.

	Response to [Ca^{2+}]$_o$			Response to L-Glu	
CPCCOEt conc.	EC_{50}	n_{Hill}	Maximal response[a]	EC_{50}	Maximal response[a]
nM	*mM*		%	*μM*	%
0	3.5	6.4	85 ± 2	1.7	100 ± 2
5	7.6	1.3	75 ± 3		
10				5.2	44 ± 8
40	14.7	1.1	60 ± 3	10.1	30 ± 10

[a] The maximal responses are normalized to the maximal response of WT mGluR1α to L-Glu.

the effect of Ro 67-4853 on the response to L-Glu, the maximal response to [Ca^{2+}]$_o$ was not changed by Ro 67-4853 (Fig. 6*B* and Table 5).

To further evaluate the effect of Ro 67-4853 on mGluR1α, HEK293 cells transiently expressing mGluR1α were preincubated with 0.5 mM Ca^{2+} and 5 nM Ro 67-4853 for up to 10 min, and then the responses to multiple concentrations of Ro 67-4853 were tested. In the presence of 0.5 mM [Ca^{2+}]$_o$, Ro 67-4853 enhanced L-Glu-induced mGluR1α activity in a concentration-dependent manner. Increasing [Ca^{2+}]$_o$ to 1.8 mM significantly increased the potency of a low dosage of Ro 67-4853 for mGluR1α ($p < 0.05$) (Fig. 6*C*). At the same time, the EC_{50} value decreased from 20.7 to 10.0 nM (Fig. 6*C* and Table 5). Interestingly, [Ca^{2+}]$_i$ oscillations were observed when the cells were treated with Ro 67-4853 (data not shown). Similar to the Ca^{2+}-sensing receptor, three different patterns of response were noted (30). Most of the cells displayed a transient spike in [Ca^{2+}]$_i$. Some cells started oscillating after the first peak, whereas others had a transient peak, and oscillations first appeared a few minutes later. When we analyzed the number of oscillating cells of the total number of responsive cells, 1.8 mM [Ca^{2+}]$_o$ significantly increased the number of oscillatory cells compared with the cells in 0.5 mM [Ca^{2+}]$_o$. The starting point of oscillation was also shifted leftward (data not shown). This suggests that [Ca^{2+}]$_o$ enhances the potency of Ro 67-4853 in activating mGluR1α.

To understand whether this modulation by [Ca^{2+}]$_o$ of the action of this allosteric modulator acting via the TMDs is indeed a result of [Ca^{2+}]$_o$ binding to the predicted [Ca^{2+}]$_o$-binding site in the ECD (*e.g.* Fig. 1), we then performed studies using an mGluR variant with a key [Ca^{2+}]$_o$-binding ligand residue mutated, E325I. Fig. 1*B* shows that Glu-325 is not directly involved in L-Glu binding, and variant E325I is able to sense L-Glu in a manner similar to WT (18). Fig. 7*A* shows that addition of 30 μM L-Glu enhanced the responsiveness of E325I to Ro 67-4853. Of note, Fig. 7*B* shows that E325I responded to 10 μM Ro 67-4853 in the absence of L-Glu in [Ca^{2+}]$_o$-free saline. Increasing [Ca^{2+}]$_o$ from 0.5 to 1.8 mM did not affect the sensitivity of E325I to Ro 67-4853, but elevating [Ca^{2+}]$_o$ increased the responses of WT mGluR1α to 300 nM Ro 67-4853 (Fig. 7*B*). This suggests that mutating the Ca^{2+}-binding site (E325I) eliminates the effect of Ca^{2+} on Ro 67-4853 but not on WT mGluR1α. To determine whether the receptors were saturated by Ro 67-4853, higher concentrations of the PAM were applied to both WT mGluR1 and E325I. As shown in Fig. 7*B*, higher concentrations of Ro 67-4853 increased the responses of both WT mGluR1 and E325I. This result suggests that [Ca^{2+}]$_o$ binding at its predicted site in the hinge region is essential for the positive allosteric action of this modulator.

DISCUSSION

In this study, we demonstrated that [Ca^{2+}]$_o$ had significant modulating effects on the actions of various orthosteric and allosteric ligands on mGuR1a as assessed using a functional readout (*i.e.* [Ca^{2+}]$_i$ responses) in receptor-transfected HEK293 cells. [Ca^{2+}]$_o$ exerted several different effects on the compounds studied here, including the orthosteric agonist L-Quis, the orthosteric antagonist (*S*)-MCPG, and allosteric modulators, *e.g.* the PAM Ro 67-4853 and the NAM CPCCOEt.

As shown in Fig. 1, the predicted [Ca^{2+}]$_o$-binding site partially overlaps the predicted orthosteric binding site for the agonist L-Quis and the antagonist (*S*)-MCPG. We have previously

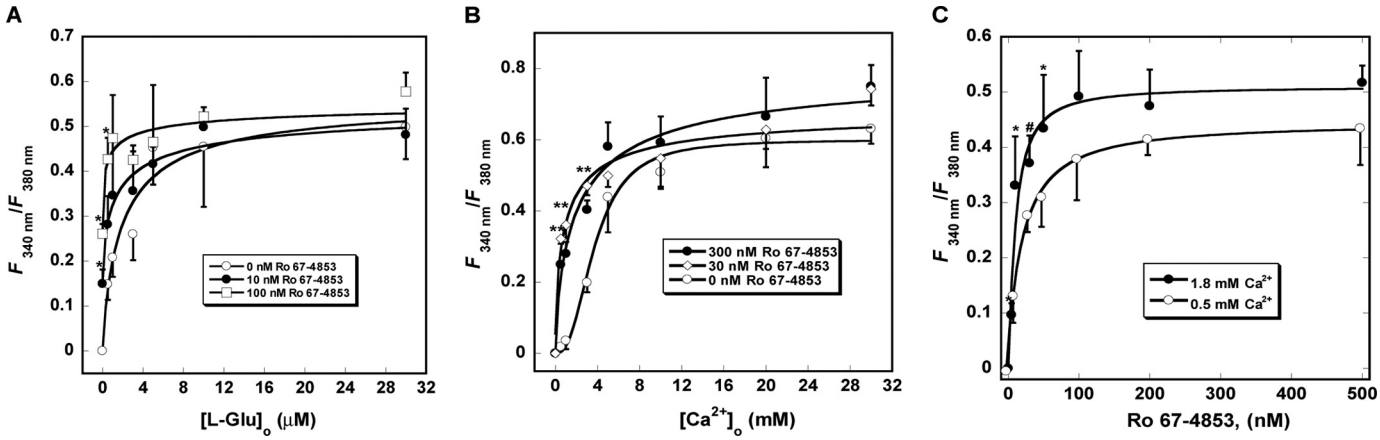

FIGURE 6. **$[Ca^{2+}]_o$ and Ro 67-4853 co-activate mGluR1α.** HEK293 cells growing on coverslips were transiently transfected with wild type mGluR1α. After dye loading, the cells were preincubated in 10 mM HEPES, 140 mM NaCl, 5 mM KCl, 0.55 mM $MgCl_2$, 0.5 mM $CaCl_2$, and 5 nM Ro 67-4853, pH 7.4 for 10 min. *A*, 10 or 100 nM Ro 67-4853 enhances the L-Glu sensitivity of mGluR1α. *B*, 30 or 300 nM Ro 67-4853 increases the $[Ca^{2+}]_o$ sensitivity of mGluR1α. *C*, addition of $[Ca^{2+}]_o$ and Ro 67-4853 to the cells. Ro 67-4853 displayed activity on mGluR1α in the presence of 0.5 mM $[Ca^{2+}]_o$, whereas 1.8 mM $[Ca^{2+}]_o$ enhanced its potency (*, $p < 0.05$; **, $p < 0.01$; #, $p = 0.05$). *Error bars* represent S.D.

TABLE 5

$[Ca^{2+}]_o$ effects on modulation of mGluR1α by Ro 67-4853 (n = 3)

WT mGluR1α was incubated with increasing concentrations (conc.) of Ro 67-4583 with either 0.5 or 1.8 mM $[Ca^{2+}]_o$ (left side) or to increasing concentrations of $[Ca^{2+}]_o$ in the presence of the indicated fixed concentrations of Ro 67-4583.

$[Ca^{2+}]_o$ conc.	EC_{50}[a]	Max. res.[b]	Ro 67-4853 conc.	EC_{50}[c]	Max. res.[b]
mM	*nM*	*%*	*nM*	*mM*	*%*
0.5	20.7	50 ± 8	0	3.5	85 ± 2
1.8	10.0	59 ± 4	30	2.1	83 ± 6
			300	0.7	83 ± 2

[a] Refers to EC_{50} of Ro 67-4853.
[b] The maximal responses (Max. res.) are normalized to the maximal response of WT mGluR1α to L-Glu.
[c] Refers to EC_{50} of Ca^{2+}.

reported the effects of $[Ca^{2+}]_o$ on $[L\text{-Glu}]_o$-induced activation of the receptor. Consistent with this, we have shown here that activation of mGluR1α by L-Quis was enhanced by $[Ca^{2+}]_o$ in a similar manner. Through binding to the Ca^{2+}-binding site on the ECD of mGluR1, $[Ca^{2+}]_o$ was capable of inducing the hydrolysis of phosphatidylinositol 4,5-bisphosphate, thus increasing inositol trisphosphate and Ca^{2+} release from the endoplasmic reticulum (18). As reported, $[Ca^{2+}]_o$ was shown to synergistically activate mGluR1α with L-Glu (18). However, activation of GPCRs is also known to induce Ca^{2+} influx through store-operated Ca^{2+} entry channels (31, 32). By utilizing Gd^{3+}, an inhibitor of these Ca^{2+} channels, we noted that mGluR1a still could induce an increase in $[Ca^{2+}]_i$ (18). But comparing this increase with the $[Ca^{2+}]_o$-induced concentration-response curve, the Gd^{3+} response after the transient increase in $[Ca^{2+}]_i$ returned the curve back to the base line (33). This suggests that Ca^{2+} release from the endoplasmic reticulum predominantly induces a transient peak, whereas Ca^{2+} influx elevates the plateau portion of the response. We also further demonstrated that increasing $[Ca^{2+}]_o$ enhanced L-Quis binding to HEK293 cells overexpressing mGluR1α, whereas the mutant E325I abolished this effect of $[Ca^{2+}]_o$ on the activation of mGluR1 (Fig. 3). Moreover, a clear difference in L-Quis and L-Glu binding was observed in the presence of physiological levels of $[Ca^{2+}]_o$. $[Ca^{2+}]_o$ in the synaptic cleft changes in the range of 0.8–1.5 mM (34), and mGluR1α is known to respond to the $[Ca^{2+}]_o$ change between 0.5 and 1.5 mM (18). Using purified ECD of mGluR1α, Jingami and co-workers (15) reported that $[Ca^{2+}]_o$ enhances the increase in Trp fluorescence induced by L-Quis and L-Glu, although $[Ca^{2+}]_o$ was reported to have no effect on L-Quis binding (35). Nash *et al.* (36) also observed that $[Ca^{2+}]_o$ produces a higher plateau $[Ca^{2+}]_i$ response and greater inositol trisphosphate accumulation in CHO cells mediated by mGluR1α, although the transient increase in $[Ca^{2+}]_i$ was not affected. Thus, our observation that $[Ca^{2+}]_o$ enhanced both L-Quis-induced $[Ca^{2+}]_i$ responses and L-Quis binding to the receptor has a physiological implication similar to the modulation by $[Ca^{2+}]_o$ of the action of L-Glu on mGluR1α. Fig. 1 shows that the predicted $[Ca^{2+}]_o$-binding site is located adjacent to the (*S*)-MCPG-binding pocket in mGluR1 in the x-ray structure (Protein Data Bank code 1ISS) that is in the hinge region of the ECD and occupies most of the residues involved in L-Glu binding (10). We tested the effects of gradually increasing concentrations of the orthosteric antagonist (*S*)-MCPG on $[Ca^{2+}]_o$-induced signaling by mGluR1α. As shown in Fig. 4, (*S*)-MCPG reduced the $[Ca^{2+}]_o$ sensitivity of mGluR1α (Fig. 4, *A* and *C*). Here we have shown that increases in the concentrations of either $[Ca^{2+}]_o$ or L-Glu overcame the inhibition induced by (*S*)-MCPG (Fig. 4). It is interesting to note that (*S*)-MCPG could not completely block the $[Ca^{2+}]_o$ sensitivity of mGluR1 (Fig. 4*C*). $[Ca^{2+}]_o$-induced responses mediated by mGluR1α were found to be only partially antagonized by (*S*)-MCPG (4). (*S*)-MCPG was shown to have the capacity to completely inhibit L-Glu-potentiated Ca^{2+}-activated Cl^- currents in *Xenopus laevis* oocytes transiently expressing mGluR1 (4). These data support our hypothesis that $[Ca^{2+}]_o$ modulates the effects of orthosteric ligands on mGluR.

The observed $[Ca^{2+}]_o$-modulated orthosteric effect is likely dependent on communication of the predicted $[Ca^{2+}]_o$-binding site with the adjacent binding site for orthosteric agonists and antagonists. We first showed that the L-Quis-binding pocket predicted here using AutoDock Vina overlaps extensively with the L-Glu-binding pocket in the reported crystal structure (Table 6). The side chain of Asp-318 is involved in both $[Ca^{2+}]_o$ and agonist binding. In our earlier study, the

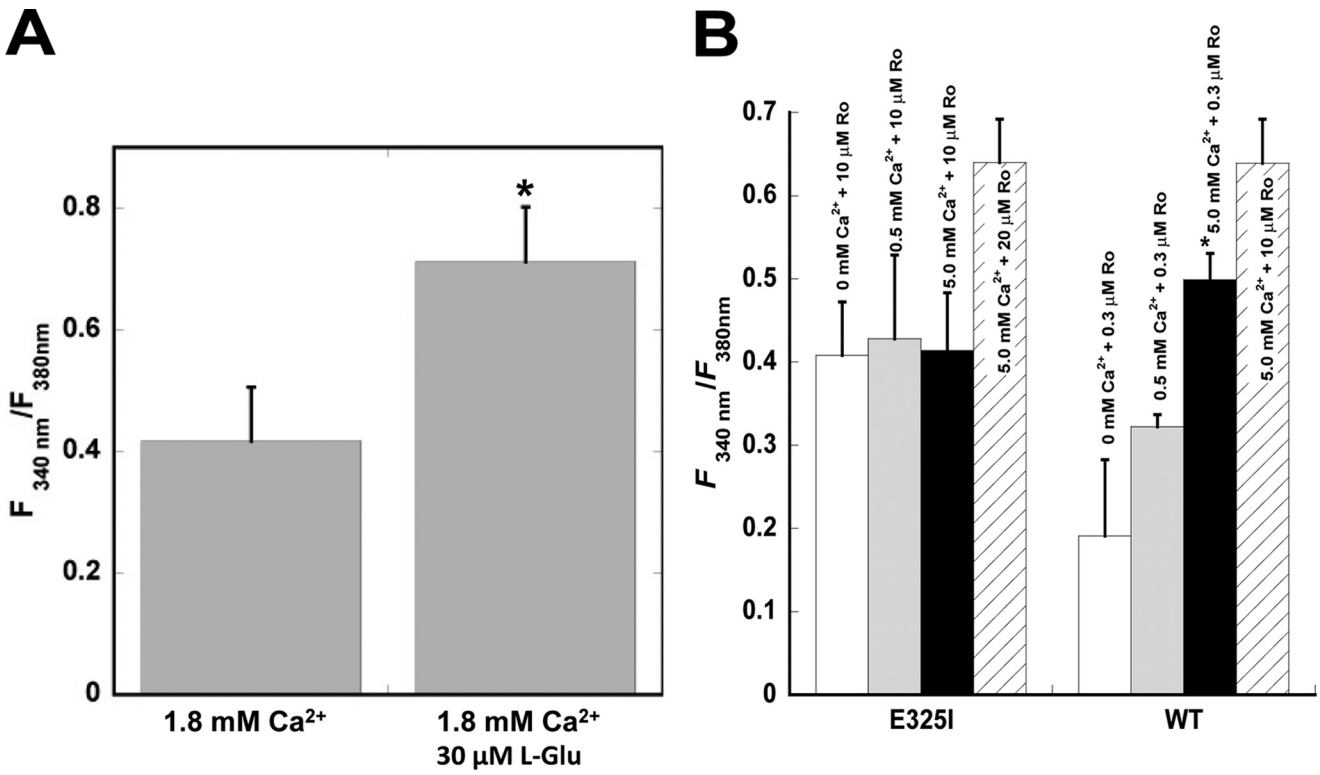

FIGURE 7. **E325I retains the enhanced responsiveness of the receptor to 10 μM Ro 67-4853 in the presence of L-Glu but loses its potentiation by $[Ca^{2+}]_o$.** *A*, addition of 30 μM L-Glu increases the Ro 67-4853 sensitivity of E325I in the presence of 1.8 mM $[Ca^{2+}]_o$ ($p = 0.014$). *B*, E325I responds to 10 μM Ro 67-4853 (*Ro*) in the absence of both $[Ca^{2+}]_o$ and L-Glu. Increasing $[Ca^{2+}]_o$ from 0 to 5.0 mM had no effect on the response of E325I to Ro 67-4853, whereas the activity of WT mGluR1 to Ro 67-4853 was progressively enhanced to increases in the $[Ca^{2+}]_i$ response of E325I ($n = 3$) (*, $p < 0.05$). Both WT mGluR1 and E325I had stronger responses to exposure to 10 and 20 μM Ro 67-4853 in the presence of 5 mM Ca^{2+}, respectively (*, $p < 0.05$). *Error bars* represent S.D.

TABLE 6

Analysis of ligand interaction by Ligand-Protein Contacts server

Protein Data Bank files bound with L-Quis, L-Glu, and (*S*)-MCPG were analyzed by the online Ligand-Protein Contacts server. The output, including distance, surface interacting, and atom number contributing to binding, were as summarized below. — indicates no contacts.

Residue number	Distance			Surface			Number of contacts		
	L-Quis	L-Glu	(*S*)-MCPG	L-Quis	L-Glu	(*S*)-MCPG	L-Quis	L-Glu	(*S*)-MCPG
	Å			Å^2					
Tyr-74	2.7	2.5	2.6	29.4	37.3	46.7	9	7	7
Arg-78	—	5.1	5.5	—	0.3	1.6	—	1	1
Trp-110	3.6	3.9	3.9	37.1	20.2	28.5	8	8	9
Gly-163	3.7	3.9	4.8	8.5	8.7	2.7	2	2	1
Ser-164	3.1	3.5	4.8	23.6	7.3	8.3	3	3	4
Ser-165	3.0	2.7	2.9	35.7	43.7	46.6	4	4	7
Ser-166	—	—	4.4	—	—	0.7	—	—	1
Ser-186	3.5	2.8	3.7	26.5	29.3	27.2	5	5	10
Ala-187	3.6	3.3	—	1.6	1.6	—	1	1	—
Thr-188	3.8	2.9	3.2	3.9	27.9	27.0	2	4	3
Ser-189	—	—	5.0	—	—	2.7	—	—	3
Asp-208	—	—	4.8	—	—	0.9	—	—	2
Tyr-236	3.6	3.4	4.2	42.9	40.4	46.7	10	14	13
Glu-292	3.9	5.0	—	22.2	5.0	—	7	5	—
Gly-293	3.7	5.1	—	25.9	1.2	—	3	1	—
Met-294	4.6	—	—	3.3	—	—	2	—	—
Asp-318	3.7	2.8	5.0	19.8	31.3	9.5	3	2	4
Gly-319	3.4	3.7	6.2	19.2	21.4	1.3	4	3	2
Arg-323	3.5	3.7	6.1	15.5	10.4	3.1	3	1	1
Lys-409	2.8	3.6	3.1	32.2	23.9	30.0	3	4	4

mutation D318I was shown to abrogate both the sensitivity to $[Ca^{2+}]_o$ and responsiveness to L-Glu (18). In this study, it also completely eliminated L-Quis-mediated activation of mGluR1 (Fig. 3*E*). This finding is supported by a previous report that the mutants T188A, D208A, Y236A, and D318A abolished the sensitivity of the receptor to both L-Quis and L-Glu, whereas the mutants R78E and R78L exhibited clearly impaired L-Quis binding (8, 9). The key residue Glu-325 is involved in $[Ca^{2+}]_o$ binding, and the mutant E325I indeed significantly impaired both the $[Ca^{2+}]_o$ and L-Glu sensitivity of the receptor (Fig. 3). On the other hand, variant D322I produced less reduction of the modulatory effects of $[Ca^{2+}]_o$ on both L-Quis and L-Glu agonist action, which is consistent with its lesser role in $[Ca^{2+}]_o$ binding with a contribution of only a main chain ligand atom (Fig. 1).

Our observed effect of $[Ca^{2+}]_o$ on responses to orthosteric agonists and antagonists of mGluR1 is consistent with molecular dynamics simulation studies performed here on the correlated motions of the hinge region in the ECD of mGluR (Fig. 2 and Table 1). We observed a strong correlation among residues in the predicted $[Ca^{2+}]_o$-binding site and residues involved in the orthosteric binding sites shared by L-Glu, L-Quis, and (*S*)-MCPG. Interestingly, mutation of the $[Ca^{2+}]_o$-binding site largely removed this correlation. Fig. 1*A* shows that the predicted $[Ca^{2+}]_o$-binding site at the hinge region is conserved in the group I mGluRs, *e.g.* mGluR1 and mGluR5 (18), calcium-sensing receptor, and T1R3, a taste receptor for $[Ca^{2+}]_o$ (37). In our previous study, $[Ca^{2+}]_o$ exhibits synergy with L-Glu in activating mGluR1α (18). We have further demonstrated here the effect of $[Ca^{2+}]_o$ in modulating orthosteric ligands that act on mGluR via communication at the hinge region of the ECD. We and others have also shown that binding of L-Phe and other amino acids to a site in the hinge region of the calcium-sensing receptor likely communicates with the predicted $[Ca^{2+}]_o$-binding site at the hinge region to increase the sensitivity of the receptor to $[Ca^{2+}]_o$ (12, 13, 38, 39). In recent years, increasing numbers of family C GPCRs have been found to exhibit synergistic modulation of the primary orthosteric agonist by allosteric modulators. Sweet enhancers binding to the hinge region of the human taste receptor are known to stabilize the active form of the receptor, thus leading to altered perception of sweet taste, whereas IMP and L-Glu also synergistically activate the umami taste receptor (40, 41). It is also interesting to note that an allosteric ligand suggested to act at the ECD domain of mGluR is located at the hinge region (42, 43). Thus, our work has strong implications for the role of the hinge region of the ECD in modulating action of small molecule ligands on family C GPCRs.

As for allosteric modulators targeting the TMDs, the binding sites of positive and negative modulators of mGluR1α are distinct (44). These allosteric modulators effectively modulate receptor activation by L-Glu, but little is known about the effects of the endogenous mineral ion Ca^{2+} on these modulators. In this study, the effects of $[Ca^{2+}]_o$ on CPCCOEt (NAM) and Ro 67-4853 (PAM) were further assessed.

The non-competitive NAM CPCCOEt is known to inhibit the L-Glu response by binding to Thr-815 and Ala-818 on the seventh transmembrane helix (45, 46). Our data shown in Fig. 5 support the contention that CPCCOEt, acting as a non-competitive inhibitor, also can diminish the $[Ca^{2+}]_i$ response of mGluR1α. Interestingly, increasing $[Ca^{2+}]_o$ restored the $[Ca^{2+}]_o$ sensitivity of the receptor. CPCCOEt not only inhibits proliferation of melanoma cells but also reverses morphine tolerance (47, 48). Thus, the findings in this study indicate that a novel drug targeting the $[Ca^{2+}]_o$-binding site in mGluR1 has the potential to tune the therapeutic effect of CPCCOEt on melanoma or addiction. Val-757 in the TMD was revealed to be critical to the activation of mGluR1 by the PAMs (27, 44). By analyzing the $[Ca^{2+}]_i$ transients and oscillations observed here, $[Ca^{2+}]_o$ not only reduced the concentration of Ro 67-4853 required to initiate $[Ca^{2+}]_i$ oscillations but also decreased the EC_{50} value and increased the maximal responses of HEK293 cells expressing mGluR1 (Fig. 6 and Table 5). In the presence of Ro 67-4853, the $[Ca^{2+}]_o$ sensitivity of mGluR1α was also enhanced, indicating an allosteric interaction between the $[Ca^{2+}]_o$-binding site and the site for Ro 67-4853. Interestingly, Ro 67-4853 only enhanced activation of mGluR1α by physiological $[Ca^{2+}]_o$ concentrations, whereas further increases in $[Ca^{2+}]_o$ abolished the Ro 67-4853 effect (Fig. 7*B*) ($p < 0.01$). This indicates that a change in $[Ca^{2+}]_o$ within the physiological range could serve as a PAM, similar to Ro 67-4853, and suggests that $[Ca^{2+}]_o$-induced enhancement of the potency of Ro 67-4853 may activate mGluR1 via the TMDs and that the activation of the TMDs could enhance the sensitivity of the receptor to agonist. Because site-directed mutagenesis suggests that Ro 67-4853 along with the other PAMs Ro 01-6128 and Ro 67-7476 likely share the same binding pocket involving Val-757. $[Ca^{2+}]_o$ could potentially enhance the potencies of other members of the Ro and VU series.

The observed modulation of the effects of PAM and NAM by $[Ca^{2+}]_o$ can be explained by the integrated action of the ECD domain with the TMDs of the receptor. This is supported by our studies using a mutation of a key $[Ca^{2+}]_o$-binding ligand residue, E325I, at the predicted $[Ca^{2+}]_o$-binding site adjacent to the L-Glu-binding site. Variant E325I markedly reduced the modulation of the action of Ro 67-4853 by $[Ca^{2+}]_o$ (Fig. 7). PAMs binding to the TMDs have been shown to enhance L-Quis binding to mGluR1α (27). It is possible that the incomplete reduction in the inhibitory effect of MCPG by $[Ca^{2+}]_o$ is due to an additional synergistic effect involving the TMD region of the receptor. By tagging the FRET pair YFP/cyan fluorescent protein to the two intracellular loops 2 (i2) of the dimeric mGluR1α, Tateyama *et al.* (49) observed that the rearrangement of the TMD induced by L-Glu was reversed by (*S*)-MCPG. Such an integrated effect of the TMD with the ECD region is further supported by studies of mGluRs with deletions of the Venus fly trap. It was found that PAMs not only potentiate the action of agonists on the full-length receptors but sometimes can display strong agonist activity on Venus fly trap-truncated receptors (50, 51). The Venus fly traps of the ECDs are not only responsible for agonist-induced activation but also prevent PAMs from activating the full-length receptor (50, 51). Taken together, our study reveals that $[Ca^{2+}]_o$ binding at the hinge region is likely to be responsible for its capacity to modulate action of other allosteric modulators. $[Ca^{2+}]_o$ at physiological levels (1.8 mM) enhanced the potency of Ro 67-4853 in modulating mGluR1α, whereas increasing $[Ca^{2+}]_o$ diminished the inhibitory effects of CPCCOEt (Figs. 5–7 and Tables 4 and 5). Over the past decade, many new PAMs and NAMs for various receptors have been developed, and the potential exists for developing allosteric modulators with greater subtype specificity than is possible for orthosteric agonists (52). The co-activation induced by endogenous agonists and PAMs binding to the hinge regions of receptors could be a common feature of family C GPCRs. These data provide further insight into the modulation of mGluR1α by $[Ca^{2+}]_o$ and suggest that $[Ca^{2+}]_o$ has the potential to modulate the profile of a variety of agents acting on mGluR1α, including agonists, antagonists, and allosteric modulators.

In conclusion, we investigated the effects of $[Ca^{2+}]_o$ on the modulation of mGluR1α by orthosteric agonists and an

orthosteric antagonist as well as by a PAM and NAM and found that $[Ca^{2+}]_o$ enhanced the actions of agonists and PAMs but attenuated the actions of antagonists and NAMs. These findings provide new insights into the targeting of mGluR1α by different classes of ligands. In addition to the specific relevance of these findings for understanding the nature of allosteric modulation of mGluR1α, they may also have general relevance for understanding the modulation of family C GPCRs by extracellular ions, such as Ca^{2+}.

Acknowledgments—We thank Stacy Schaefer, William Watkins, Stefanie Ritter, and Kevin Paavola at Emory University for technical advice; Chen Zhang and Jie Feng at Georgia State University and Aldebaran Hofer from Harvard Medical School for discussion and suggestions; and Doug Sheffler at Vanderbilt University for advice.

REFERENCES

1. Neyman, S., and Manahan-Vaughan, D. (2008) Metabotropic glutamate receptor 1 (mGluR1) and 5 (mGluR5) regulate late phases of LTP and LTD in the hippocampal CA1 region in vitro. *Eur. J. Neurosci.* **27,** 1345–1352
2. Lavreysen, H., Janssen, C., Bischoff, F., Langlois, X., Leysen, J. E., and Lesage, A. S. (2003) [^{3}H]R214127: a novel high-affinity radioligand for the mGlu1 receptor reveals a common binding site shared by multiple allosteric antagonists. *Mol. Pharmacol.* **63,** 1082–1093
3. Lindsley, C. W., Wisnoski, D. D., Leister, W. H., O'brien J. A., Lemaire, W., Williams, D. L., Jr., Burno, M., Sur, C., Kinney, G. G., Pettibone, D. J., Tiller, P. R., Smith, S., Duggan, M. E., Hartman, G. D., Conn, P. J., and Huff, J. R. (2004) Discovery of positive allosteric modulators for the metabotropic glutamate receptor subtype 5 from a series of N-(1,3-diphenyl-1H-pyrazol-5-yl)benzamides that potentiate receptor function *in vivo*. *J. Med. Chem.* **47,** 5825–5828
4. Kubo, Y., Miyashita, T., and Murata, Y. (1998) Structural basis for a Ca^{2+}-sensing function of the metabotropic glutamate receptors. *Science* **279,** 1722–1725
5. Whang, P. G., O'Hara, B. J., Ratliff, J., Sharan, A., Brown, Z., and Vaccaro, A. R. (2008) Pseudarthrosis following lumbar interbody fusion using bone morphogenetic protein-2: intraoperative and histopathologic findings. *Orthopedics* **31,** pii
6. Yuan, K., Jing, G., Chen, J., Liu, H., Zhang, K., Li, Y., Wu, H., McDonald, J. M., and Chen, Y. (2011) Calmodulin mediates Fas-induced FADD-independent survival signaling in pancreatic cancer cells via activation of Src-extracellular signal-regulated kinase (ERK). *J. Biol. Chem.* **286,** 24776–24784
7. Chen, Y., Zhou, Y., Lin, X., Wong, H. C., Xu, Q., Jiang, J., Wang, S., Lurtz, M. M., Louis, C. F., Veenstra, R. D., and Yang, J. J. (2011) Molecular interaction and functional regulation of connexin50 gap junctions by calmodulin. *Biochem. J.* **435,** 711–722
8. Levant, J. A., Walsh, J. H., and Isenberg, J. I. (1973) Stimulation of gastric secretion and gastrin release by single oral doses of calcium carbonate in man. *N. Engl. J. Med.* **289,** 555–558
9. Sato, T., Shimada, Y., Nagasawa, N., Nakanishi, S., and Jingami, H. (2003) Amino acid mutagenesis of the ligand binding site and the dimer interface of the metabotropic glutamate receptor 1. Identification of crucial residues for setting the activated state. *J. Biol. Chem.* **278,** 4314–4321
10. Tsuchiya, D., Kunishima, N., Kamiya, N., Jingami, H., and Morikawa, K. (2002) Structural views of the ligand-binding cores of a metabotropic glutamate receptor complexed with an antagonist and both glutamate and Gd^{3+}. *Proc. Natl. Acad. Sci. U.S.A.* **99,** 2660–2665
11. Nagar, B., Overduin, M., Ikura, M., and Rini, J. M. (1996) Structural basis of calcium-induced E-cadherin rigidification and dimerization. *Nature* **380,** 360–364
12. Huang, Y., Zhou, Y., Castiblanco, A., Yang, W., Brown, E. M., and Yang, J. J. (2009) Multiple Ca^{2+}-binding sites in the extracellular domain of the Ca^{2+}-sensing receptor corresponding to cooperative Ca^{2+} response. *Biochemistry* **48,** 388–398
13. Huang, Y., Zhou, Y., Yang, W., Butters, R., Lee, H. W., Li, S., Castiblanco, A., Brown, E. M., and Yang, J. J. (2007) Identification and dissection of Ca^{2+}-binding sites in the extracellular domain of Ca^{2+}-sensing receptor. *J. Biol. Chem.* **282,** 19000–19010
14. Tabata, T., Aiba, A., and Kano, M. (2002) Extracellular calcium controls the dynamic range of neuronal metabotropic glutamate receptor responses. *Mol. Cell. Neurosci.* **20,** 56–68
15. Suzuki, Y., Moriyoshi, E., Tsuchiya, D., and Jingami, H. (2004) Negative cooperativity of glutamate binding in the dimeric metabotropic glutamate receptor subtype 1. *J. Biol. Chem.* **279,** 35526–35534
16. Wang, X., Kirberger, M., Qiu, F., Chen, G., and Yang, J. J. (2009) Towards predicting Ca^{2+}-binding sites with different coordination numbers in proteins with atomic resolution. *Proteins* **75,** 787–798
17. Wang, X., Zhao, K., Kirberger, M., Wong, H., Chen, G., and Yang, J. J. (2010) Analysis and prediction of calcium-binding pockets from apo-protein structures exhibiting calcium-induced localized conformational changes. *Protein Sci.* **19,** 1180–1190
18. Jiang, Y., Huang, Y., Wong, H. C., Zhou, Y., Wang, X., Yang, J., Hall, R. A., Brown, E. M., and Yang, J. J. (2010) Elucidation of a novel extracellular calcium-binding site on metabotropic glutamate receptor 1α (mGluR1α) that controls receptor activation. *J. Biol. Chem.* **285,** 33463–33474
19. Kunishima, N., Shimada, Y., Tsuji, Y., Sato, T., Yamamoto, M., Kumasaka, T., Nakanishi, S., Jingami, H., and Morikawa, K. (2000) Structural basis of glutamate recognition by a dimeric metabotropic glutamate receptor. *Nature* **407,** 971–977
20. Case, D. A., Darden, T. A., Cheatham, I., T. E., Simmerling, C. L., Wang, J., Duke, R. E., Luo, R., Crowley, M., Walker, R. C., Zhang, W., Merz, K. M., Wang, B., Hayik, S., Roitberg, A., Seabra, G., Kolossváry, I., Wong, K. F., Paesani, F., Vanicek, J., Wu, X., Brozell, S. R., Steinbrecher, T., Gohlke, H., Yang, L., Tan, C., Mongan, J., Hornak, V., Cui, G., Mathews, D. H., Seetin, M. G., Sagui, C., Babin, V., and Kollman, P. A. (2008) *AMBER 10*, University of California, San Francisco
21. Jorgensen, W. L., Chandrasekhar, J., Madura, J. D., Impey, R. W., and Klein, M. L. (1983) Comparison of simple potential functions for simulating liquid water. *J. Chem. Phys.* **79,** 926–935
22. Cornell, W. D., Cieplak, P., Christopher, I. B., Gould, I. R., Merz, J. K. M., Ferguson, D. M., Spellmeyer, D. C., Fox, T., Caldwell, J. W., and Kollman, P. A. (1995) A second generation force field for the simulation of proteins, nucleic acids and organic molecules. *J. Am. Chem. Soc.* **117,** 5179–5197
23. Urmi, D., and Hamelberg, D. (2009) Reoptimization of the AMBER force field parameters for peptide bond (ω) torsions using accelerated molecular dynamics. *J. Phys. Chem.* **113,** 16590–16595
24. Darden, T., York, D., and Pedersen, L. (1993) Particle mesh Ewald—an N·log(N) method for Ewald sums in large systems. *J. Chem. Phys.* **98,** 10089–10092
25. Ryckaert, J. P., Ciccotti, G., and Berendsen, H. J. (1977) Numerical integration of the Cartesian equations of motion of a system with constraints: molecular dynamics of *n*-alkanes. *J. Comput. Phys.* **23,** 327–341
26. Hepler, R. W., Grimm, K. M., Nahas, D. D., Breese, R., Dodson, E. C., Acton, P., Keller, P. M., Yeager, M., Wang, H., Shughrue, P., Kinney, G., and Joyce, J. G. (2006) Solution state characterization of amyloid β-derived diffusible ligands. *Biochemistry* **45,** 15157–15167
27. Nemeth, E. F., Steffey, M. E., Hammerland, L. G., Hung, B. C., Van Wagenen, B. C., DelMar, E. G., and Balandrin, M. F. (1998) Calcimimetics with potent and selective activity on the parathyroid calcium receptor. *Proc. Natl. Acad. Sci. U.S.A.* **95,** 4040–4045
28. Harrington, P. E., and Fotsch, C. (2007) Calcium sensing receptor activators: calcimimetics. *Curr. Med. Chem.* **14,** 3027–3034
29. Litschig, S., Gasparini, F., Rueegg, D., Stoehr, N., Flor, P. J., Vranesic, I., Prézeau, L., Pin, J. P., Thomsen, C., and Kuhn, R. (1999) CPCCOEt, a noncompetitive metabotropic glutamate receptor 1 antagonist, inhibits receptor signaling without affecting glutamate binding. *Mol. Pharmacol.* **55,** 453–461
30. Huang, Y., Zhou, Y., Wong, H. C., Castiblanco, A., Chen, Y., Brown, E. M., and Yang, J. J. (2010) Calmodulin regulates Ca^{2+}-sensing receptor-mediated Ca^{2+} signaling and its cell surface expression. *J. Biol. Chem.* **285,** 35919–35931

31. Putney, J. W., Jr. (1986) A model for receptor-regulated calcium entry. *Cell Calcium* **7,** 1–12
32. Parekh, A. B., and Putney, J. W., Jr. (2005) Store-operated calcium channels. *Physiol. Rev.* **85,** 757–810
33. Abe, H., Tateyama, M., and Kubo, Y. (2003) Functional identification of Gd^{3+} binding site of metabotropic glutamate receptor 1α. *FEBS Lett.* **545,** 233–238
34. Vassilev, P. M., Mitchel, J., Vassilev, M., Kanazirska, M., and Brown, E. M. (1997) Assessment of frequency-dependent alterations in the level of extracellular Ca^{2+} in the synaptic cleft. *Biophys. J.* **72,** 2103–2116
35. Selkirk, J. V., Price, G. W., Nahorski, S. R., and Challiss, R. A. (2001) Cell type-specific differences in the coupling of recombinant mGlu1α receptors to endogenous G protein sub-populations. *Neuropharmacology* **40,** 645–656
36. Nash, M. S., Saunders, R., Young, K. W., Challiss, R. A., and Nahorski, S. R. (2001) Reassessment of the Ca^{2+} sensing property of a type I metabotropic glutamate receptor by simultaneous measurement of inositol 1,4,5-trisphosphate and Ca^{2+} in single cells. *J. Biol. Chem.* **276,** 19286–19293
37. Dorr, P., Westby, M., Dobbs, S., Griffin, P., Irvine, B., Macartney, M., Mori, J., Rickett, G., Smith-Burchnell, C., Napier, C., Webster, R., Armour, D., Price, D., Stammen, B., Wood, A., and Perros, M. (2005) Maraviroc (UK-427,857), a potent, orally bioavailable, and selective small-molecule inhibitor of chemokine receptor CCR5 with broad-spectrum anti-human immunodeficiency virus type 1 activity. *Antimicrob. Agents Chemother.* **49,** 4721–4732
38. Conigrave, A. D., Mun, H. C., and Lok, H. C. (2007) Aromatic L-amino acids activate the calcium-sensing receptor. *J. Nutr.* **137,** Suppl. 1, 1524S–1527S
39. Zhang, Z., Qiu, W., Quinn, S. J., Conigrave, A. D., Brown, E. M., and Bai, M. (2002) Three adjacent serines in the extracellular domains of the CaR are required for L-amino acid-mediated potentiation of receptor function. *J. Biol. Chem.* **277,** 33727–33735
40. Zhang, F., Klebansky, B., Fine, R. M., Liu, H., Xu, H., Servant, G., Zoller, M., Tachdjian, C., and Li, X. (2010) Molecular mechanism of the sweet taste enhancers. *Proc. Natl. Acad. Sci. U.S.A.* **107,** 4752–4757
41. Zhang, F., Klebansky, B., Fine, R. M., Xu, H., Pronin, A., Liu, H., Tachdjian, C., and Li, X. (2008) Molecular mechanism for the umami taste synergism. *Proc. Natl. Acad. Sci. U.S.A.* **105,** 20930–20934
42. Acher, F. C., Selvam, C., Pin, J. P., Goudet, C., and Bertrand, H. O. (2011) A critical pocket close to the glutamate binding site of mGlu receptors opens new possibilities for agonist design. *Neuropharmacology* **60,** 102–107
43. Ogawa, H., Qiu, Y., Philo, J. S., Arakawa, T., Ogata, C. M., and Misono, K. S. (2010) Reversibly bound chloride in the atrial natriuretic peptide receptor hormone-binding domain: possible allosteric regulation and a conserved structural motif for the chloride-binding site. *Protein Sci.* **19,** 544–557
44. Hemstapat, K., de Paulis, T., Chen, Y., Brady, A. E., Grover, V. K., Alagille, D., Tamagnan, G. D., and Conn, P. J. (2006) A novel class of positive allosteric modulators of metabotropic glutamate receptor subtype 1 interact with a site distinct from that of negative allosteric modulators. *Mol. Pharmacol.* **70,** 616–626
45. Rodriguez, A. L., Nong, Y., Sekaran, N. K., Alagille, D., Tamagnan, G. D., and Conn, P. J. (2005) A close structural analog of 2-methyl-6-(phenylethynyl)-pyridine acts as a neutral allosteric site ligand on metabotropic glutamate receptor subtype 5 and blocks the effects of multiple allosteric modulators. *Mol. Pharmacol.* **68,** 1793–1802
46. Bräuner-Osborne, H., Jensen, A. A., and Krogsgaard-Larsen, P. (1999) Interaction of CPCCOEt with a chimeric mGlu1b and calcium sensing receptor. *Neuroreport* **10,** 3923–3925
47. Haas, H. S., Pfragner, R., Siegl, V., Ingolic, E., Heintz, E., Schraml, E., and Schauenstein, K. (2007) The non-competitive metabotropic glutamate receptor-1 antagonist CPCCOEt inhibits the *in vitro* growth of human melanoma. *Oncol. Rep.* **17,** 1399–1404
48. Smith, F. L., Smith, P. A., Dewey, W. L., and Javed, R. R. (2004) Effects of mGlu1 and mGlu5 metabotropic glutamate antagonists to reverse morphine tolerance in mice. *Eur. J. Pharmacol.* **492,** 137–142
49. Tateyama, M., Abe, H., Nakata, H., Saito, O., and Kubo, Y. (2004) Ligand-induced rearrangement of the dimeric metabotropic glutamate receptor 1α. *Nat. Struct. Mol. Biol.* **11,** 637–642
50. El Moustaine, D., Granier, S., Doumazane, E., Scholler, P., Rahmeh, R., Bron, P., Mouillac, B., Banères, J. L., Rondard, P., and Pin, J. P. (2012) Distinct roles of metabotropic glutamate receptor dimerization in agonist activation and G-protein coupling. *Proc. Natl. Acad. Sci. U.S.A.* **109,** 16342–16347
51. Goudet, C., Gaven, F., Kniazeff, J., Vol, C., Liu, J., Cohen-Gonsaud, M., Acher, F., Prézeau, L., and Pin, J. P. (2004) Heptahelical domain of metabotropic glutamate receptor 5 behaves like rhodopsin-like receptors. *Proc. Natl. Acad. Sci. U.S.A.* **101,** 378–383
52. Wang, L., Martin, B., Brenneman, R., Luttrell, L. M., and Maudsley, S. (2009) Allosteric modulators of G protein-coupled receptors: future therapeutics for complex physiological disorders. *J. Pharmacol. Exp. Ther.* **331,** 340–348